Case Reports in Oncology

Case Rep Oncol 2022;15:918–926
DOI: 10.1159/000525174
Received: April 23, 2022
Accepted: May 12, 2022
Published online: November 8, 2022

Case Report

Adult T-Cell Leukemia-Lymphoma Presenting Concurrently with Myelopathy

Sneha Poondru[a] Ancy Joseph[b] John C. Harding[b]
Hemalatha Sundaramoorthi[b] Neha Mehta-Shah[b]
Patrick Green[c] Anjum Hassan[d] Daniel A. Rauch[b] Lee Ratner[b]

[a]School of Medicine, University of Missouri-Kansas City, Kansas City, MO, USA; [b]Division of Oncology, Washington University School of Medicine, St Louis, MO, USA; [c]Center for Retrovirus Research and Department of Veterinary Biosciences, The Ohio State University, Columbus, OH, USA; [d]Department of Pathology & Immunology, Washington University School of Medicine, St Louis, MO, USA

Keywords
Adult T-cell leukemia/lymphoma · HTLV-associated myelopathy/tropical spastic paresis · Brentuximab-vedotin

Abstract
Human T-cell leukemia virus type 1 (HTLV-1) is an oncogenic retrovirus. Of the approximate ten to twenty million people currently infected worldwide, 4–9% of infected individuals develop adult T-cell leukemia/lymphoma (ATLL) or HTLV-associated myelopathy/tropical spastic paresis (HAM/TSP) in their lifetime. The current report is based on a patient who presented concurrently with CD30+ lymphoma subtype ATLL and HAM/TSP. The patient's ATLL responded to brentuximab-vedotin-based chemotherapy; however, HAM/TSP did not improve. The patient's peripheral blood mononuclear cells were cultured and injected into immunodeficient mice, and the mice developed massive organ involvement and chronic lymphocytic leukemia-subtype ATLL. This case study is novel in the findings of concurrent development of ATLL and HAM/TSP, the response to brentuximab-vedotin chemotherapy, and the use HTLV-1 helix basic zipper protein-targeted probe for RNAscope for diagnosis.

Sneha Poondru and Ancy Joseph contributed equally to this work.

Correspondence to:
Lee Ratner, lratner@wustl.edu

Case Rep Oncol 2022;15:918–926
DOI: 10.1159/000525174

Introduction

Human T-cell leukemia virus type 1 (HTLV-1) is an oncogenic retrovirus that is endemic in southern Japan, the Caribbean, South America, parts of Africa, and Iran [1]. Approximately ten to twenty million individuals are infected worldwide. Approximately 5% of infected individuals will develop adult T-cell leukemia/lymphoma (ATLL), and 0.25–4% will develop HTLV-associated myelopathy/tropical spastic paresis (HAM/TSP). Although most viral gene expression is silenced when ATLL develops, the HTLV-1 helix basic zipper (HBZ) gene is continuously expressed at all stages of infection [2]. Here, we describe a novel case of a patient presenting concurrently with CD30+ ATLL and HAM/TSP, who responded to brentuximab-vedotin chemotherapy regimen. The diagnosis was confirmed with a novel HBZ RNAscope assay.

Case Presentation

A 51-year-old African-American woman, born in the Midwest with no relevant travel history, with a past medical history of diet-controlled diabetes mellitus type 2, alcohol abuse, pancreatitis, anemia, osteoarthritis, gastric ulcers, and gastroesophageal reflux disease, presented with a 1-month history of progressive and profound lower extremity weakness and mild numbness. She reported inability to walk and severe back pain, bowel and bladder incontinence, 20 pound weight loss, drenching night sweats, fevers, chills, chest pain, and dyspnea. Laboratory studies were remarkable for a lactate dehydrogenase value of 507 U/L (ULN 250 U/L), as well as normal thyroid studies, vitamin B12 level, and negative infectious studies including syphilis and HIV, except positive results for antibodies to HTLV-1 (Table 1). Cerebrospinal fluid (CSF) showed 79 mg/dL protein and 42 nucleated cell (94% mature lymphocytes) but negative cytology and negative paraneoplastic antibody studies. HTLV-1 proviral load (PVL) in the CSF was 0.09 copies/mononuclear cell (Table 2). HTLV-1 antibodies were also detected in the CSF (Table 1).

Chest computerized tomography revealed a 9.4 × 4.2-cm right hilar mass extending from the mediastinum to the right and left paratracheal and subcarinal regions, obliterating the right upper and middle lobe bronchi, which was fluorodeoxyglucose (FDG) positive on positron emission tomography (PET) (Fig. 1a). Hypermetabolic supraclavicular and mesenteric nodes were also noted. An MRI of cervical, thoracic, and lumbar spine showed a faint area of T2/STIR

Table 1. HTLV-1 antibody titers

Sample	Dilution	Mean OD	Abritrary unit × dilution factor
Plasma	1:500	1.29	37,200
	1:50	2.51[a]	N/A
CSF	1:500	0.08[a]	N/A
	1:50	0.45	750

[a]Denotes out of the linear range of the assay. HTLV-1-specific antibody response was quantified in cerebrospinal fluid (CSF) and plasma using an Avioq HTLV-1/2 Microelisa System (Avioq, Inc., Research Triangle Park, NC, USA). CSF and plasma samples were diluted 1:5, followed by either a 1:50 or 1:500 dilution. Dilutions that resulted in mean absorbance values within the linear range provided by the serially diluted positive control of the kit were interpolated and assigned an arbitrary unit. Values were multiplied by the appropriate dilution factor.

Case Rep Oncol 2022;15:918–926
DOI: 10.1159/000525174

Table 2. HTLV-1 PVLs[a]

	Tissue	PVL (copies/mononuclear cell)
Baseline	Blood	0.18
Completion of treatment	Blood	0.06
Baseline	CSF	0.09
PBMC in culture	Blood	0.76
PDX-1	Spleen	4.49
PDX-2	Spleen	10.34

[a]DNA was extracted from peripheral blood mononuclear cells (PBMC) and mouse samples using DNeasy Kits (Qiagen). HTLV proviral load (PVL) was measured using the digital droplet (dd) PCR method. In brief, PCR was performed using Bio-Rad 2x ddPCR super mix for probes, with two set of specific primers and probes for HTLV-1 provirus (TAX) and human gene encoding the RNAse P enzyme (RPP 30). Droplets were generated using the QX 200 droplet generator, and PCR was performed and analyzed using the QX 200 droplet reader. The PVL was calculated as [(copy number of HTLV-TAX)/(copy number of RPP 30/2)]. All samples were run in duplicates, and averages were taken.

hyper-intense signal within the cervical cord at C2-C4, with additional possible areas of involvement at T1-T3, concerning for a demyelinating condition. The lower extremity paralysis and bowel and bladder incontinence were ascribed to HTLV-1-associated myelopathy (HAM).

Bronchoscopic biopsy of the paratracheal lymph node showed a diffuse infiltrate of atypical medium to large CD3+CD4+CD30+ T-cells, negative for CD1, CD10, anaplastic lymphoma kinase-1 (ALK-1), and Epstein-Barr virus encoded RNA-1 and near complete loss of CD5 and CD7, with rare nonneoplastic CD20 cells (Fig. 2a–e). The atypical T cells had irregular nuclear contours and high nuclear-to-cytoplasmic ratio, prominent nucleoli, increased apoptosis, mitotic figures, and foci of necrosis, resulting in the diagnosis of Lugano stage IIIB ATLL, lymphoma subtype [3].

Her initial course was complicated by deep venous thrombosis, pulmonary embolus, and cardiogenic shock, requiring an intravenous filter and anticoagulation. Electromyography showed severe loss of compound muscle action potentials and absent sensory nerve action potentials in the legs. She was treated with six cycles of brentuximab-vedotin, cyclophosphamide, doxorubicin, and prednisone (BV-CHP), complicated by febrile neutropenia in the first cycle, *Escherichia coli* urosepsis during the fifth cycle, and pneumonia during the sixth cycle. Following chemotherapy, she continued to have urinary tract infections and oral candidiasis and lower limb paralysis. Repeat PET scan showed significant improvement in mediastinal lymphadenopathy with no residual FDG avidity but new multifocal lesions in the cerebrum and cerebellum (Fig. 1b). However, a brain MRI showed no lesions and no leptomeningeal enhancement.

The diagnosis was confirmed by RNAscope showing foci of HBZ RNA in the patient's lymphoma cells (Fig. 2f). Negative control results were obtained with a nonspecific RNAscope probe (*E. coli* dapB) (Fig. 2g), and positive control results were obtained with a RNAscope probe (human PPIB) directed against a constitutively expressed cellular RNA (Fig. 2h).

Immunodeficient NSG-Kit mice were inoculated with a short-term culture of peripheral blood mononuclear cells (PBMCs) from the patient, which had a PVL of 0.76 copies/mL (Table 2). After 8 and 9 weeks, respectively, the mice experienced weight loss and dehydration and were sacrificed. Necropsy revealed massive hepatosplenomegaly, tumor infiltration into the lungs, and enlarged brachial and inguinal nodes. Both mice had elevated leukocyte counts

Case Rep Oncol 2022;15:918–926
DOI: 10.1159/000525174

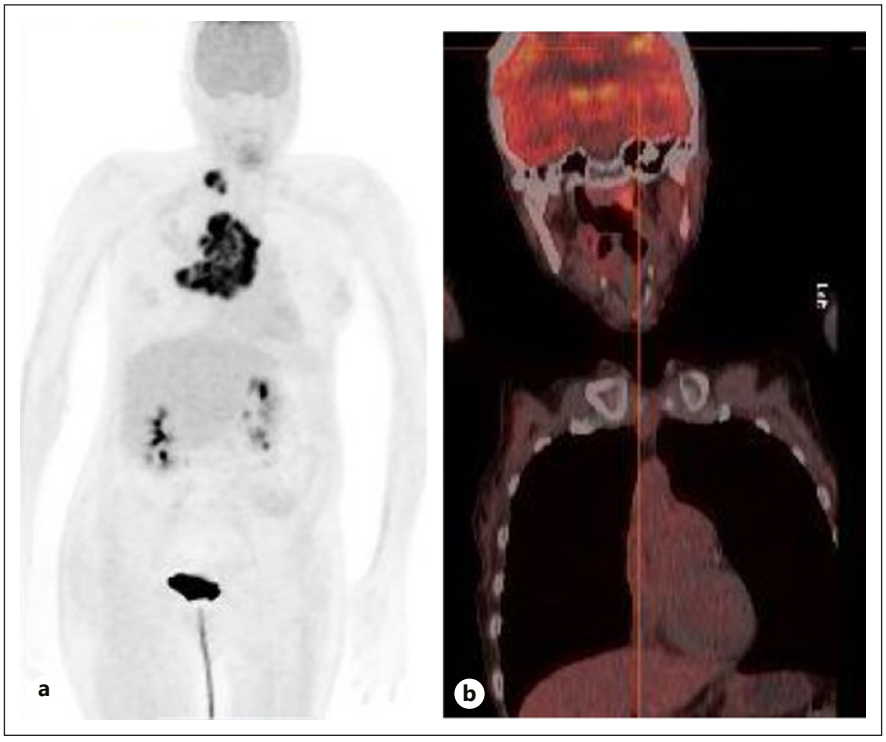

Fig. 1. PET scans before and after treatment. **a** PET/CT performed prior to treatment showed a large infiltrative mediastinal mass which was encasing the trachea and bronchi, with obliteration of the lumen of the right upper and middle lobe bronchi. The mass extended along the right paratracheal region. There was a conglomerate of right supraclavicular lymph nodes which demonstrated markedly increased metabolic activity. The mass extended to the left aspect of the trachea and into the aortopulmonary window as well as the subcarinal region. The maximum SUV was 13.8. This uptake was markedly greater than liver, consistent with a 5PS = 5. Resultant airspace opacities were seen distal to the areas of bronchial compression, which did not demonstrate increased FDG uptake. This likely represented postobstructive pneumonia. Right middle lobe collapse was seen. The mass was seen on the prior contrast-enhanced CT to be attenuating and compressing the right pulmonary arterial tree. An enlarged mesenteric lymph node was seen which measured 1.9 cm, with a maximum SUV of 7.3. An additional smaller hypermetabolic 1-cm mesenteric lymph node was seen inferiorly. Additional CT findings included diffuse body wall edema, calcifications in the left hemithyroid, a moderate right pleural effusion, and an evolving left lower lobe infarct were noted, without substantially increased metabolic activity. **b** PET scan after completion of therapy showed a new focus of increased activity along the left frontoparietal cerebrum, as well as within the central cerebellum along the posterior aspect of the fourth ventricle. There was near-resolution of extensive consolidation and pleural effusion of the right lung, with a few scattered areas of residual right upper lobe consolidation. Extensive cavitary change in the anterior segment right upper lobe corresponded to healed areas of prior necrotizing pneumonia. Mediastinal soft tissue centered in the subcranal region had resolved. There was no focus of residual increased activity, other than linear prevertebral metabolic activity which corresponded to the esophagus. New mildly increased activity of both L2 and to lesser extent within the tonsils, as well as because of the anterior lower oral cavity were likely inflammatory. Mildly increased activity at the gastroesophageal junction suggested focal esophagitis. There was new marked increased activity corresponding to areas of irregular thickening of the bladder base, suggesting severe cystitis. A 4-cm photopenic defect in the left bladder had no corresponding finding on a prior CT, suggesting new development of an intraluminal mass, which was most consistent with thrombus. Focal increased activity at the left sacral ulcer site was seen. A brain MRI obtained at that time showed scattered T2/FLAIR hyperintensities, compatible with chronic small vessel disease. No areas of abnormal contrast enhancement were seen.

Case Rep Oncol 2022;15:918–926
DOI: 10.1159/000525174

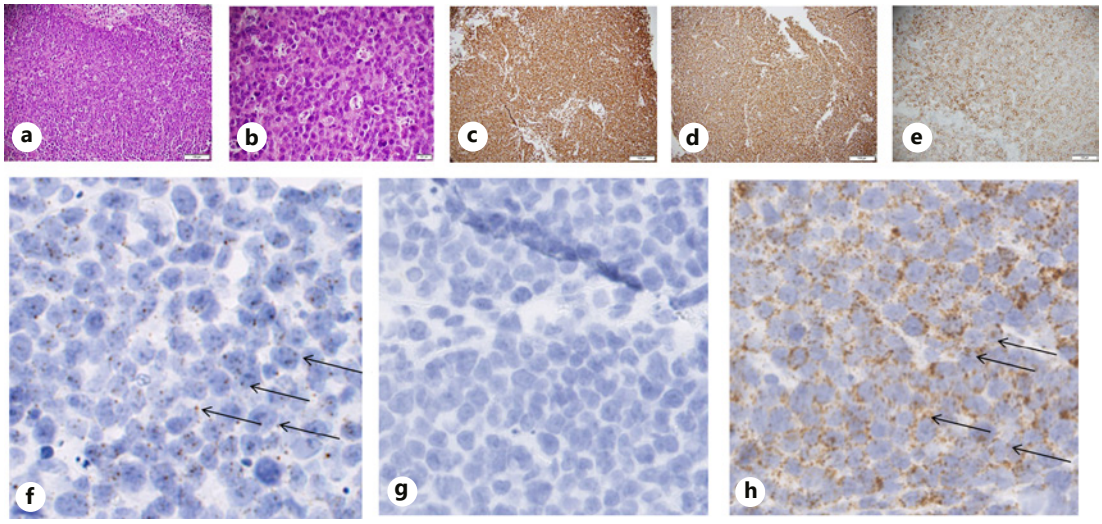

Fig. 2. Pathological findings of the anterior mediastinal mass. Sections of the right paratracheal 4R lymph node obtained at bronchoscopy showed (**a**) partial effacement of nodal architecture by a diffuse infiltrate consisting of (**b**) medium to large sized atypical cells with irregular nuclear contours, high nuclear to cytoplasmic ratio, and occasional prominent nucleoli. The neoplastic cells showed focal sinusoidal infiltration. The background showed increased apoptosis, mitotic figures, and foci of necrosis. Flow cytometry showed 27% of total events within the designated lymphocyte gate, 95% of which were CD3 positive T cells which showed a CD4-to-CD8 ratio of more than 10:1 with no significant coexpression of CD4 and CD8 among T cells. The abnormal T cells were positive for cytoplasmic CD3, CD30 (64%), and CD45 (bright), negative for TdT, and showed retained expression of CD2, and near complete loss of expression of CD5 and CD7. CD1 and CD10 were negative. Immunostains were performed to characterize staining of cells in tissue context. The neoplastic infiltrate was diffusely positive for (**c**) CD3 and (**d**) CD4 and showed coexpression of CD2 and (**e**) CD30 with significant loss of CD5 and CD7 expression. Immunostains for ALK-1, TdT, CD1a, and ISH-EBER were negative. CD20 highlighted small nonneoplastic B cells mainly with a follicular distribution. **f** RNAscope was positive (arrows) with an HBZ probe, (**g**) negative with non-expressed bacterial dihydrodipicolinate reductase B probe, and (**h**) positive with a constitutively expressed human peptidyl-prolyl cis-trans isomerase B probe. Formalin-fixed, paraffin-embedded tissues were used for in situ hybridization using RNAscope (ADC Biotechnology), according to the manufacturer's protocol. In brief, 4–5-μm thick sections were prepared from patient samples and baked at 60°C for 1 h followed by deparffinization and pretreatments. Hybridization was performed at 40°C for 2 h using HybeZ hybridization oven using an HBZ specific probe (targeting nucleotides 173–1,363 in the HBZ RNA) or a positive (Hs-PIPB, targeting human housekeeping gene) or negative (DapB) control probe. Amplification and detection of signals were followed accordingly and the sections were counter stained using hematoxylin. Images were taken using a Nanozoomer digital slide scanner (Hamamatsu Photonics).

(10.3 K/mm^3 and 15.2 K/mm^3). Blood smears revealed abnormal large and small lymphocytes with convoluted nuclei (Fig. 3a–h). FACS analysis revealed human CD4+CD45+ cells in the spleen, lung, liver, bone marrow, and peripheral blood, with a mixture of single and double CD4- and CD8-positive cells (Fig. 3i–k). Sequence analyses of PDX lymphoma tissue showed identical polymorphisms to those present in the patient (i.e., lymphoma was patient-derived) and oligoclonal integration of the HTLV-1 provirus (Fig. 3l) with oligoclonal indices of 0.41 and 0.43. On a scale of 0–1, 0 represents polyclonal integration, and 1.0 represents monoclonal integration. The recurrent CARD11 R423W substitution described by Kataoka et al. [4] was present in PDX-derived cells (2.4% and 4.1%) but only found in 0.08% of reads in the patient's PBMC-derived DNA.

Consistent with the clinical course of lymphoma, the HTLV-1 PVL in the peripheral blood decreased after treatment from 0.18 to 0.06 (Table 2). However, after activation and expansion

Case Rep Oncol 2022;15:918–926
DOI: 10.1159/000525174

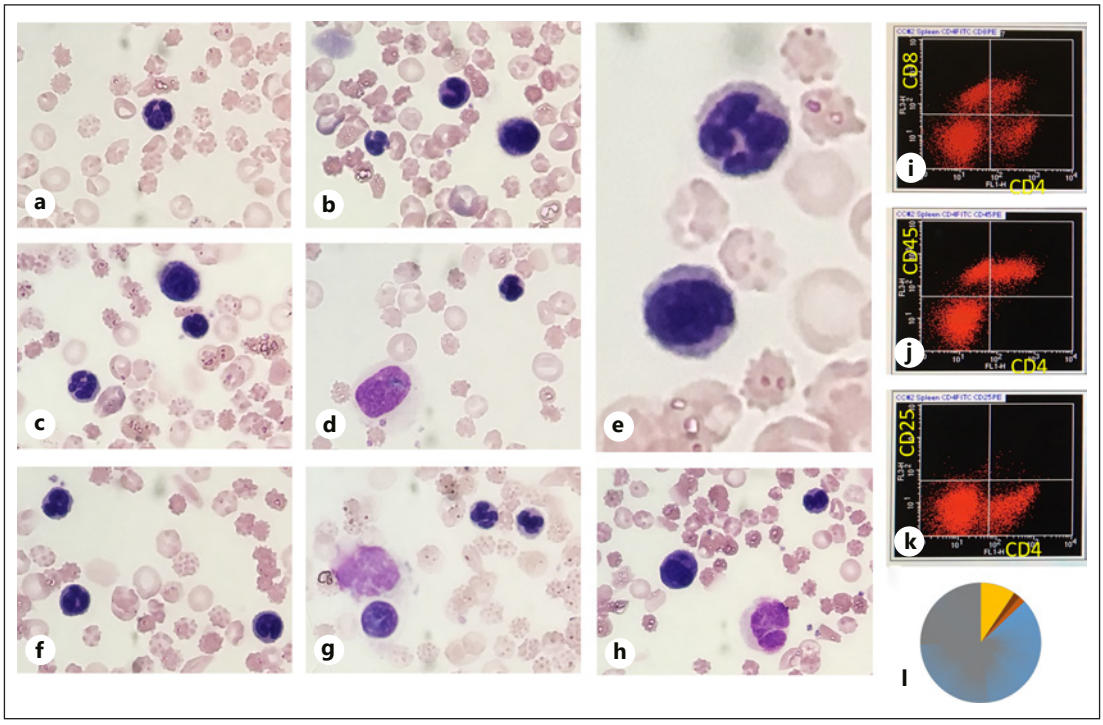

Fig. 3. PDX model of ATLL with patient peripheral blood lymphocytes. Short-term cultured PBMCs from the patient were injected into two NSG-Kit mice. After 8 and 9 weeks, respectively, the mice lost weight and were sacrificed and necropsy was performed. **a–h** Blood smears exhibited abnormal large and small cells, many of which had highly lobulated nuclei. (**i–k**) Mice exhibited massive splenomegaly, and FACS analysis of splenocytes showed a mixture of single- and double-positive CD4+ and CD8+ lymphocytes. PBMCs from the patient were collected at baseline and grown for 14 days in RPMI-1640 medium supplemented with 10% fetal calf serum, 4 mM glutamine, 50 μg/mL penicillin and streptomycin, 50 units/mL interleukin 2, and 25 μL/mL of human CD3/CD28 T-cell activator reagent (ImmunoCult; Stem Cell Technologies, Cambridge, MA, USA). FACS analysis of cultured cells confirmed expansion of T cells with approximately equal numbers of CD4 and CD8 cells by day 5. After 14 days in culture, 5 million cultured cells from the patient were injected intraperitoneal into each of two NSG-Kit mice (Jackson Labs). Mice were sacrificed after 8 and 9 weeks, respectively, when weight loss and dehydration was first noted, and necropsy performed. All animal studies were performed in accordance with research protocols approved by the Institutional Animal Care and Use Committee (IACUC; Animal Welfare Assurance #A-3381-01) at Washington University. (**l**) Clonal abundance of unique integration sites within tumor of one of the mice is shown. DNA obtained from fresh PBMCs obtained before and after therapy as well as splenocytes from two PDX mice were submitted to the McDonnell Genome Institute at Washington University for Illumina sequencing after probe capture to detect somatic variants that recurrently emerge in ATLL. At 2,000–5,000 coverage, this method had the power to detect somatic variants present in ATLL clones if the clone represents more than 0.1–0.25% of the sample.

in culture ex vivo in the presence of anti-CD3/CD28 and IL-2, the PVL increased significantly to 0.76 and increased even more dramatically in the splenocytes of the PDX mice (4.49 and 10.34).

Discussion/Conclusion

The patient was seropositive for HTLV-1 and presented concurrently with ATLL and HAM/TSP. Although she did not have spasticity, which is typically associated with HAM/TSP, she did have the characteristic progressive weakness of bilateral lower extremities and

urinary disturbances [5]. CSF analyses for malignancy, paraproteins, and biomarkers of multiple sclerosis were negative in this patient. The patient's PET scan after completion of chemotherapy showed new multifocal lesions in the cerebrum and cerebellum, which are more consistent with HAM/TSP than cerebral lymphoma, in light of the negative brain MRI findings. Other less likely considerations for her paraplegia were nutritional deficiency, a paraneoplastic syndrome, myelitis from another virus, and amyotrophic lateral sclerosis, but laboratory studies were negative for these disorders.

This case is notable because HAM/TSP rarely presents concurrently with ATLL, most likely due to the fact that each disorder develops in only 0.25–5% of individuals at some time in their lifetime. The current therapy for ATLL with glucocorticoid and cytotoxic agents may have therapeutic activity for HAM/TSP, but our patient did not show improvement in her progressive myelopathy after chemotherapy treatment. In contrast, a therapeutic antibody against CCR4, mogamulizumab, has reported activities in both ATLL and HAM/TSP [6]. However, this agent was not available at the time of presentation of our patient.

Previous case reports described instances of ATLL developing after HAM/TSP diagnosis, with very few showing HAM/TSP after or concurrent with ATLL presentation [7]. Takeda et al. [7] described a 5-year prospective cohort study of 527 HAM/TSP patients and described ATLL prevalence and incidence in this cohort of 3.0% and 3.8 cases per 1,000-person-years of follow-up, respectively. Genomic analysis revealed somatic mutations of HTLV-1-infected cells in 90% of these individuals, and 11% of them had dominant clones and developed ATLL during the observation period [4, 7]. Similar observations were made in a prospective cohort of HTLV-1-infected patients, including individuals with HAM/TSP, who subsequently developed ATLL [8].

The patient described in the current report received a regimen of BV-CHP. Brentuximab-vedotin is an antibody-drug conjugate directed against CD30. She was given BV-CHP rather than cyclophosphamide, doxorubicin, vincristine, and prednisone based on the results from the ECHELON-2 clinical trial [9]. This was a randomized, placebo-controlled trial comparing BV-CHP with standard-of-care cyclophosphamide, doxorubicin, vincristine, and prednisone in CD30+ mature peripheral T-cell lymphoma in 452 eligible subjects, resulting in median progression-free survival of 48 versus 21 months, febrile neutropenia in 18% versus 15%, and peripheral neuropathy in 52% versus 55%, respectively. The multicenter trial only had four cases of CD30+ ATLL out of 226 patients receiving BV-CHP, so there is limited evidence of the therapy in this context. Two ongoing studies in refractory T-cell lymphomas include ATLL patients [10].

The patient's posttreatment PET scan showed complete resolution of mediastinal, supraclavicular, and mesenteric lymphadenopathy with no residual FDG avidity, indicating successful anti-lymphoma therapy. Due to the patient's resistance to hospitalization, she was not a candidate for allogeneic hematopoietic cell transplantation. Zidovudine and interferon alpha are often used concurrently with chemotherapy [11]. However, since it is unclear whether or not this improves response rates or overall survival and likely increases the toxicity of the regimen, it was not considered for this patient. Although zidovudine and interferon alpha are active in the acute subtype of ATLL, there is very little activity in the lymphoma subtype [12].

The PDX mouse studies provide support for the diagnosis of ATLL (Fig. 3). The finding of "chronic lymphocytic leukemia (CLL)-type" ATLL has been described [13], with small cells, no nucleoli, and a clumped chromatin pattern. CLL-type ATLL is thought to be a disorder of immature lymphocytes with a less aggressive course and a chronic disease. The patient did not have characteristic ATLL "flower" cells in the peripheral blood nor did she have leukemia. However, lymphoma cells circulating in the peripheral blood of this patient, expanded in culture and in NSG mouse xenografts, revealed small cells with highly lobulated nuclei similar to CLL-type ATLL, and carried highly elevated HTLV-1 PVLs. The PVL is increased with

Case Rep Oncol 2022;15:918–926
DOI: 10.1159/000525174

severity in HAM/TSP and is high in patients with rapid progression [14]. A PVL of 0.18 copies/PBMC at clinical presentation is consistent with a highly aggressive HAM/TSP.

The diagnosis of ATLL is determined by both clinical and laboratory features. HTLV-1 serology is a required test. To detect monoclonal integration of the HTLV-1 provirus genome, Southern blot analysis or inverse PCR may be done. However, these methods are time-consuming. ATLL is often misdiagnosed as various other mature T-cell malignancies, including mycosis fungoides and Sezary syndrome, cerebriform variants of T-cell prolymphocytic leukemia, peripheral T-cell lymphoma, unspecified (PTCL-U), angioimmunoblastic T-cell lymphoma, or Hodgkin's lymphoma. PTCL-U and ATLL are usually difficult to differentiate due to similar morphology, and thus, the presence of HTLV in the cells is essential to differentiate the two disorders.

The HTLV-1 provirus genome consists of the *gag, pol*, and *env* genes. The TAX protein is an important viral factor in the pathogenesis of ATLL, but recent studies have reported that TAX expression is undetectable in about 60% of ATLL cases. Additionally, the frequency of transcription of the *tax* gene is very low and could only be detected by RT-PCR, not Western blot analysis. Although TAX expression decreases, another important HTLV-1 protein, HBZ, is expressed throughout the course of disease. A previous study showed that HBZ transcript detection by in situ hybridization of formalin-fixed, paraffin-embedded patient biopsy sections is an accurate, reliable way to diagnose ATLL by confirming the presence of the virus in the malignant cells [15]. HBZ RNA expression was detected by RNAscope in tumor cells. Although this method does not detect HTLV clonality, it does not require cells to be cultured and thus provides an easy, useful histological diagnostic test for ATLL, especially in sero-indeterminate patients or in cases with atypical pathological or clinical features. Takatori et al. [15] described the identification of HTLV-1-infected cells in 17 of 18 ATLL cases. When combined with the use of HTLV-1 PCR assays, they found 100% sensitivity in distinguishing ATLL from non-ATLL cases in HTLV-1 carriers [15].

This case report and data from a PDX model and HBZ RNAscope of the patient's samples demonstrate methods to improve diagnosis and outcomes by making clinicians and pathologists more aware of ATLL. Moreover, response to brentuximab-vedotin in this CD30+ ATLL mediastinal tumor highlights a new approach to therapy. The co-occurrence of HAM/TSP represents an interesting and unusual feature in this patient.

Statement of Ethics

Written informed consent was obtained from the patient for publication of this case report and any accompanying images. This study protocol was reviewed and approved by the Institutional Review Board of Washington University School of Medicine, approval number 201104376.

Conflict of Interest Statement

The authors have no conflicts of interest to declare.

Funding Sources

This study was funded by Public Health Service grants from the National Cancer Institute. Funders had no role in study design, data collection and analysis, decision to publish, or preparation of the manuscript.

Author Contributions

Sneha Poondru and Lee Ratner wrote the manuscript, and Ancy Joseph, John C. Harding, Hemalatha Sundaramoorthi, Neha Mehta-Shah, Patrick Green, Anjun Hassan, and Daniel A. Rauch performed experiments or provided patient management. Sneha Poondru, Ancy Joseph, John C. Harding, Hemalatha Sundaramoorth, Neha Mehta-Shah, Patrick Green, Anjum Hassan, Daniel A. Rauch, and Lee Ratner approved the manuscript.

Data Availability Statement

This study includes no supplementary material. All data that support the findings of this study are included in this article. Further inquiries can be directed to the corresponding author.

References

1 Gessain A, Cassar O. Epidemiological aspects and world distribution of HTLV-1 infection. Front Microbiol. 2012;3:388. https://doi.org/10.3389/fmicb.2012.00388.:article
2 Matsuoka M, Mesnard J-M. HTLV-1 bZIP factor; the key viral gene for pathogenesis. Retrovirology. 2020;17(1):2. https://doi.org/10.1186/s12977-020-0511-0.
3 Shimoyama M. Diagnostic criteria and classification of clinical subtypes of adult T-cell leukemia-lymphoma: a report from the Lymphoma Study Group. Br J Hematol. 1991;79(3):428–37. https://doi.org/10.1111/j.1365-2141.1991.tb08051.x.
4 Kataoka K, Nagata Y, Kitanaka A, Shiraishi Y, Shimamura T, Yasunaga J I, et al. Integrated molecular analysis of adult T-cell leukemia/lymphoma. Nat Genet. 2015;47(11):1304–15. https://doi.org/10.1038/ng.3415.
5 Yamano Y, Sato T. Clinical pathophysiology of human T-lymphotropic virus-type 1-associated myelopathy/tropical spastic paraparesis. Front Microbiol. 2012;3:389. https://doi.org/10.3389/fmicb.2012.00389.
6 Sato T, Coler-Reilly ALG, Yagishita N, Araya N, Inoue E, Furuta R, et al. Mogamulizumab (anti-CCR4) in HTLV-1-associated myelopathy. N Engl J Med. 2018;378(6):529–38. https://doi.org/10.1056/NEJMoa1704827.
7 Takeda R, Ishigaki T, Ohno N, Yokoyama K, Kawamata T, Fukuyama T, et al. Immunophenotypic analysis of cerebrospinal fluid reveals concurrent development of ATL in the CNS of a HAM/TSP patient. Int J Hematol. 2020;111(6):891–6. https://doi.org/10.1007/s12185-019-02815-7.
8 Rowan A G, Dillon R, Witkover A, Melamed A, Demontis M-A, Gillet N A, et al. Evolution of retrovirus-infected premalignant T-cell clones prior to adult T-cell leukemia/lymphoma diagnosis. Blood. 2020;135(23):2023–32. https://doi.org/10.1182/blood.2019002665.
9 Horwitz S, O'Connor OA, Pro B, Illidge T, Fanale M, Advani R, et al. Brentuximab vedotin with chemotherapy for CD30-positive peripheral T-cell lymphoma (ECHELON-2): a global, double-blind, randomised, phase 3 trial. Lancet. 2019;393(10168):229–40. https://doi.org/10.1016/S0140-6736(18)32984-2.
10 Katsuya H, Ishitsuka K. Treatment advances and prognosis for patients with adult T-cell leukemia-lymphoma. J Clin Exp Hemeatop. 2017;57(3):87–97. https://doi.org/10.3960/jslrt.17008.
11 Hodson A, Crichton S, Montoto S, Mir N, Matutes E, Cwynarski K, et al. Use of zidovudine and interferon alfa with chemotherapy improves survival in both acute and lymphoma subtypes of adult T-cell leukemia/lymphoma. J Clin Oncol. 2011;29(35):4696–701. https://doi.org/10.1200/JCO.2011.35.5578.
12 Bazarbachi A, Suarez F, Fields P, Hermine O. How I treat adult T-cell leukemia/lymphoma. Blood. 2011;118(7):1736–45. https://doi.org/10.1182/blood-2011-03-345702.
13 Tsukasaki K, Imaizumi Y, Tawara M, Fujimoto T, Fukushima T, Hata T, et al. Diversity of leukaemic cell morphology in ATL correlates with prognostic factors, aberrant immunophenotype and defective HTLV-1 genotype. Br J Haematol. 1999;105(2):369–75. https://doi.org/10.1111/j.1365-2141.1999.01323.x.
14 Olindo S, Lezin A, Cabre P, Merle H, Saint-Vil M, Kaptue ME, et al. HTLV-1 proviral load in peripheral blood mononuclear cells quantified in 100 HAM/TSP patients: a marker of disease progression. J Neurol Sci. 2005;237(1–2):53–9. https://doi.org/10.1016/j.jns.2005.05.010.
15 Takatori M, Sakihama S, Miyara M, Imaizumi N, Miyagi T, Ohshiro K, et al. A new diagnostic algorithm using biopsy specimens in adult T-cell leukemia/lymphoma: combination of RNA in situ hybridiation and quantitative PCR for HTLV-1. Mod Pathol. 2021;34(1):51–58. https://doi.org/10.1038/s41379-020-0635-8.